



# Journal of Applied and Computational Mechanics



Research Paper

## Thermal Performance of Oscillating Blade with Various Geometries in a Straight Channel

Ehsan Izadpanah<sup>1</sup>, Milan Yazdani<sup>2</sup>, Mohamad Hamed Hekmat<sup>3</sup>, Yasser Amini<sup>4</sup>

<sup>1</sup> Department of Mechanical Engineering, Persian Gulf University, Bushehr 75169, Iran, Email: e.izadpanah@pgu.ac.ir

<sup>2</sup> South Pars Gas Company, Bushehr 75391/311, Iran, Email: milan\_yazdani@yahoo.com

<sup>3</sup> Department of Mechanical Engineering, Tafresh University, Tafresh 39518-79611, Iran, Email: hekmat@tafreshu.ac.ir

<sup>4</sup> Department of Mechanical Engineering, Persian Gulf University, Bushehr 75169, Iran, Email: aminiyasser@pgu.ac.ir

Received November 30 2019; Revised February 12 2020; Accepted for publication March 10 2020.

Corresponding author: E. Izadpanah (e.izadpanah@pgu.ac.ir)

© 2022 Published by Shahid Chamran University of Ahvaz

**Abstract.** In this study, the effect of stationary and oscillating blades on the forced convection heat transfer in a channel is studied numerically. Simulations are performed in a fully-developed, laminar, unsteady, and incompressible flow with Reynolds number and Prandtl number equal to 100 and 1, respectively. The effects of the blade geometry, oscillating speed and oscillation angle on heat transfer and pressure drop are studied. The results are presented in terms of time-averaged Nusselt number, temperature, and vorticity distribution and the pressure drop. The results indicate that the oscillation angle, oscillating speed of the blade, and the number of the blades, affect the thermal performance of the channel. In most cases, it is observed that the effect of the oscillation angle is more than that for the oscillating speed on heat transfer enhancement. However, increasing the number of blades does not necessarily help to enhance the heat transfer, but it can slightly decrease the pressure drop.

**Keywords:** Convection heat transfer, Oscillating blade, Blade configuration, Pressure drop, Vortex shedding.

### 1. Introduction

Because of increases in energy systems, high-density heat flux dissipation is recently interested in many pieces of research and has various industrial applications such as electronic chip, photovoltaic cells, high-power microwave devices, and vehicle batteries. Heat transfer enhancement technique can be used to design more efficient heat exchangers, which play a significant role in the energy system size and performance, controlling indirect emission of greenhouse gases, global warming, and ozone depletion.

Methods of heat transfer enhancement can be classified into two categories: active and passive [1]. Passive methods do not require external energy; rather heat transfer can be increased by modifying the surface shape [2], roughing the surface [3], using extended surfaces [4], adding vortex generators [5, 6], and inserts [7], modifying fluid properties by adding solid particles [8-10] or using the effects of vortex-induced vibration [11-13]. However, in the active method, external energy such as electrostatic field, acoustic vibration, injection, mechanical auxiliary devices (stir fluids by mechanical instruments or rotation of the pipe surface) and surface or fluid vibration is being used, which can be utilized with proper efficiency to enhance heat and mass transfer.

Over the last decades, various and extensive researches have been done in the field of the active methods of heat transfer enhancement. Khan et al. [14] numerically investigated the mixed convection heat transfer in a rectangular channel equipped with a variable speed rotational cylinder. The effects of the speed and direction of rotation of the cylinder as well as the Reynolds number on flow pattern, isothermal lines, and average and local Nusselt numbers were studied. The results showed that the direction of rotation and angular velocity of the cylinder has a significant effect on the temperature distribution and heat transfer characteristics. Esmaeilzadeh et al. [15] investigated the application of the electro-hydrodynamic actuators as an active method. The main focus was on the effect of the electric field intensity on the thermal performance in the wide range of Reynolds numbers. The results indicated that for the flow with Reynolds number less than 1000, single wire-plate electrode is suitable for enhancing the local heat transfer. By increasing the number of wires to three, it would be possible to use this method for turbulent flow up to the Reynolds number 2000. Eid and Gomaa [16] experimentally examined the effect of the vibration of the thin planner fins on the heat transfer enhancement. The fins were heated by an electric heater and vibrated at a frequency between 12.5 to 50 Hz. They concluded that vibration at higher frequencies is more effective. Raguraman et al. [17] experimentally



investigated the effect of geometric parameters on the heat transfer coefficient for agitated vessels. In this research, the effect of important design parameters such as type of stirrer, angle and shape of the blades and its position were investigated and optimized. The results showed that these parameters have same effect on the overall heat transfer coefficient, but the speed of the blade is most effective. Page et al. [18] numerically studied the natural convection heat transfer from the counter-rotating cylinders in a tandem arrangement. They found that by increasing the Rayleigh number, the optimum distance between the cylinders is reduced, and also the heat transfer rate for optimized structures enhances with increasing the rotational speed. According to the results, the heat transfer rate of the rotating cylinders enhances compared to that of stationary ones. Beskok et al. [19] simulated the convection heat transfer of the uniformly heated walls of a straight channel in the presence of a rotationally oscillating adiabatic cylinder. The study was conducted to find the proper angle of rotation and the effects of the frequency on the heat transfer. They found that the vortex dynamics, the thermal boundary layer thickness and Prandtl number play an important role in increasing heat transfer. It was observed that formation of high-intensity vortices close to the channel wall is highly desirable since it caused the flow rotation and, as a result, the displacement of the hot fluid near the wall and the cold fluid in the center of the channel. It was also found that by increasing the oscillation frequency of the cylinder to more than 0.85 normal frequencies of the vortex shedding, the heat transfer decreases, but as the oscillation angle increases, heat transfer enhances continuously. Léal et al. [20] investigated the main techniques for increasing the heat transfer between the solid wall and fluid for single-phase and two-phase systems. They also studied the techniques that used the time-periodic variations of the wall. They indicated that these variations in the wall, by disrupting the boundary layer, increases the heat transfer. Pourgholam et al. [21] investigated enhancing the heat transfer in a channel equipped with the rotating and oscillating blades in an angular direction. Their main focus was on studying the effect of the angular velocity of the rotation and oscillation of the blades as well as the Prandtl number on heat transfer. They concluded that the increase in heat transfer for the oscillating blade and the stationary blade is more than other cases in Reynolds number 50 and 100, respectively. Yeom et al. [22] experimentally simulated the piezoelectric translational agitator with high frequency oscillating blades in a channel equipped with the micro pin-fins, and studied its effect on increasing heat transfer. The results showed a 25% enhancement in heat transfer compared to that in a non-agitator channel. Izadpanah et al. [23] numerically studied the effect of rotating and oscillating blade motion on increasing the heat transfer of Newtonian and non-Newtonian fluid in a channel. Non-Newtonian fluid under investigation was purely viscous and was modeled using the power-law relationship. The results showed that, depending on the power law index range, stationary or oscillating blade have more influence on the heat transfer enhancement. It was also observed that by increasing the power law index, the amount of heat transfer decreases. It was concluded that the presence of the blade for all the fluid indexes has a positive effect on enhancing the heat transfer. Kankariya et al. [24] experimentally investigated the effect of rotational speed of an impeller on the improvement of heat transfer mechanically fluidized reactor. They indicated that the overall heat transfer coefficient increases with the increment of the rotational speed.

Although several works have been done in the field of active methods, there are very few researches studying the effect of oscillating blades with different configurations on the heat transfer in microchannels. The main objective of this research is to investigate the effect of using the oscillating blades on increasing the heat transfer in a channel, which can be used in micro-electro-mechanical-systems (MEMS). Accordingly, the main focus is to investigate the effect of number of blades on the amount of heat transfer and pressure drop to achieve the optimum configuration with respect to the straight channel. In addition, the effect of the angle and the speed of oscillation of the blades on vortex shedding pattern and, finally, the enhancement of the heat transfer and pressure drop are studied.

## 2. Theoretical Formulation

In this section, first the problem under investigation is defined. In the following, the governing equations are presented. The boundary conditions of the problem, including the boundary condition of the velocity and temperature at the flow inlet and outlet and on the walls, are introduced in this section. In the end, the used non-dimensional parameters are defined.

### 2.1 Problem statement

Numerical results are presented for two-dimensional ( $b \gg 3D$ ), incompressible, laminar, and unsteady Newtonian fluid flow for 26 different test cases. First case is a straight channel (without blade) and 2 to 6 geometries are channels equipped with blades with different geometrical shapes (Fig. (a) to (e)) which will be studied for stationary and oscillating states. Also, the results are compared with the results of the channel including stationary and oscillating blade type **■** and the stationary and oscillating circular cylinder which were previously studied in [21]. The constant heat flux condition is applied to the upper and lower walls of the channel. The blade with length  $D$  is located at the distance  $4D$  from the inlet of the channel, and can be stationary or oscillating in angular direction. Blockage ratio (the ratio of the blade size to the width of the channel) is  $1/3$ , and the channel length is  $31D$ .

### 2.2 Flow field governing equations

Considering the above assumptions and assuming that the thermodynamic properties of the fluid are constant, and regardless of the buoyancy force and the term of viscous dissipation, the conservation equations of mass, momentum and energy are as follows:

$$\nabla \cdot \vec{u} = 0, \quad (1)$$

$$\rho \left( \frac{\partial \vec{u}}{\partial t} + (\vec{u} \cdot \nabla) \vec{u} \right) = -\nabla p + \mu \nabla^2 \vec{u}, \quad (2)$$

$$\rho c_p \left( \frac{\partial T}{\partial t} + \vec{u} \cdot \nabla T \right) = k \nabla^2 T, \quad (3)$$



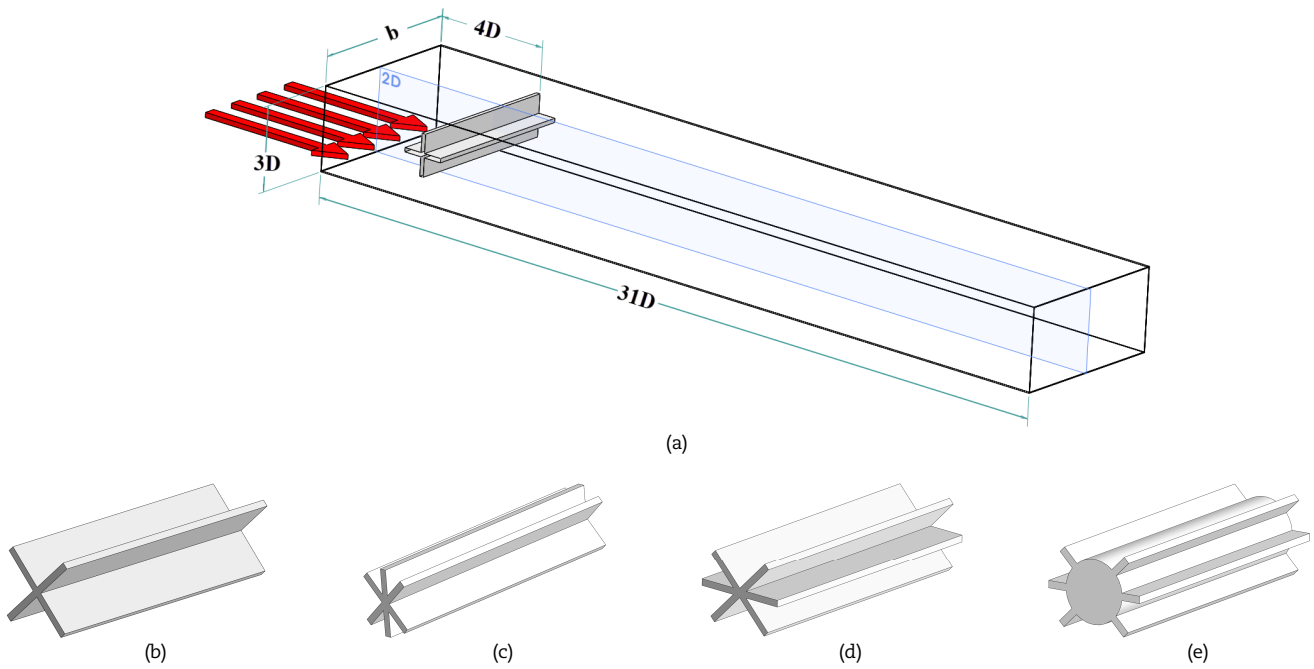


**Fig. 1.** Schematic of (a) geometry of the channel with blade type + and different configurations of blade (b) ✕, (c) ✖, (d) ✗, (e) ✙ (the diameter of the middle cylinder is 7/8D)

where  $\vec{u}, \rho, t, p, \mu, c_p, T$  and  $k$  are the velocity vector with  $u_x$  and  $u_y$  components, density, time, pressure, dynamic viscosity, specific heat, temperature and thermal conductivity of the fluid, respectively.

**2.3 Boundary conditions**

At the inlet, the flow is considered to be fully developed hydrodynamically with constant temperature:

$$u_{x,in} = 1.5u_{x,m} \left[ 1 - \left( \frac{y}{1.5D} \right)^2 \right], u_{y,in} = 0, T = T_\infty, \tag{4}$$

where  $u_{x,in}, u_{y,in}$  and  $T_\infty$  are the mean velocity of the fluid along  $x$  and  $y$  directions and free stream temperature, respectively. On the walls of the channel for velocity, the no-slip boundary condition and for the temperature, the boundary condition of the constant flux is applied. On the surface of the blades, the no-slip and the adiabatic boundary conditions are considered. At the outlet, the opening boundary conditions, allowing the fluid to cross the boundary surface in either direction, are used.

**2.4 Non-dimensional parameters**

One of the important parameters for evaluating the heat transfer rate from the upper and lower walls to the fluid is the overall time averaged Nusselt number  $\overline{Nu}$ . To determine this parameter, first, the local Nusselt number  $Nu(x,t)$  is calculated as follows:

$$Nu(x,t) = \frac{q'' D_h}{k (T_w(x,t) - T_b(x,t))} \tag{5}$$

where  $q'', D_h$  and  $T_w$  are respectively thermal flux, hydraulic diameter and wall temperature. The bulk temperature  $T_b$  is defined as follows:

$$T_b = \frac{\int u_x T dy}{\int u_x dy} \tag{6}$$

As a result, the time averaged Nusselt number of the wall during each period of blade oscillation is determined as follows:

$$\overline{Nu}(x) = \frac{1}{\tau} \int Nu(x,t) dt \tag{7}$$

where  $\tau$  is the period of the oscillating blade. Finally, the overall time averaged Nusselt number, which is the spatial average of the Nusselt number obtained from Eq. (7) along the channel, is evaluated as follows:

$$\overline{Nu} = \frac{1}{L} \int \overline{Nu}(x) dx \tag{8}$$



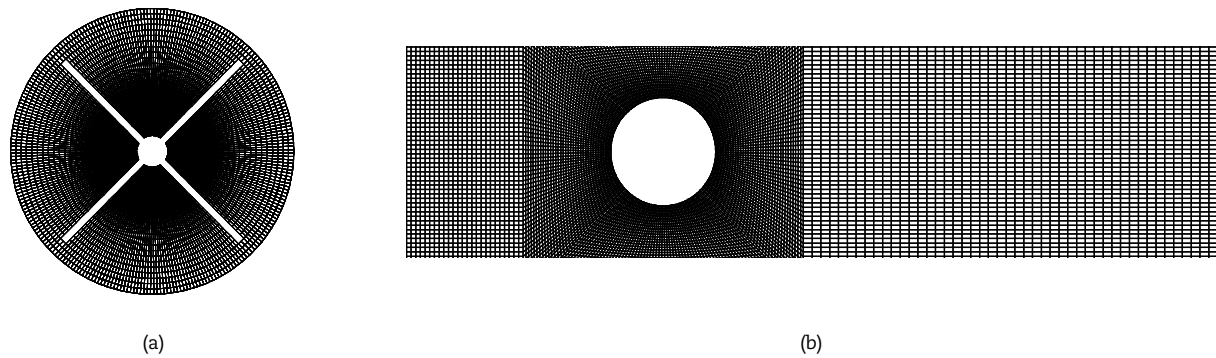


Fig. 2. Grid generated by the sliding mesh method (a) oscillating and (b) stationary domain

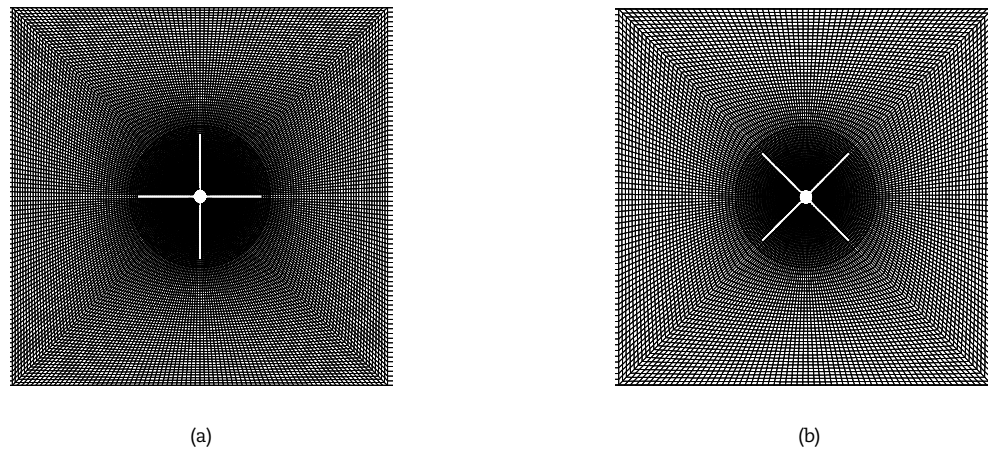


Fig. 3. Grid shown for  $\theta = \pi / 4$  at five different times of blades movement  $t =$  (a)  $0, \tau/2, \tau$  and (b)  $\tau/4, 3\tau/4$

where  $L$  is the length of channel. The Reynolds number  $Re$  and Prandtl number  $Pr$  for the Newtonian fluids are also defined as follows:

$$Re = \frac{\rho u_m D_h}{\mu} \quad (9)$$

$$Pr = \frac{c_p \mu}{k} \quad (10)$$

### 3. Numerical Considerations

This section deals with the numerical solution of the problem. The discretization method of the governing equations, the accuracy of the parameters, the utilized grid, grid independency and numerical validation are expressed.

#### 3.1 Numerical method

Numerical results are obtained using ANSYS CFX software [25]. This software uses the element-based finite volume method to solve the governing equations. A high-resolution scheme is used to discrete the advection terms. Moreover, the implicit second order backward scheme is utilized to investigate the problem in unsteady state. The computational time step is chosen  $10^{-4}$  seconds, which is 0.01 of minimum time required for an oscillation period of the blade. The convergence criterion of simulation (based on the root mean square of residual) is considered  $5 \times 10^{-6}$ . For this value, the convergence of some variables (such as velocity, temperature, and pressure) in the desired point and consequently relevant integrated quantities such as overall Nusselt number is achieved. Moreover, lowering this criterion does not change the results.

To investigate oscillating blade in angular direction, there is a need for a grid that has the minimum deviation or elongation during the rotation. Therefore, the sliding mesh method is applied. The used grid for all the cases is in accordance with Fig. 2, which consists of two rotating (Fig. 2 (a)) and stationary (Fig. 2 (b)) regions. As shown in Fig. 3. The moving region rotates and transfers the information to the stationary region through the middle layer. It can be seen that this grid does not have any deformation, both oscillating and stationary grids are slipped on each other, the grid overlap does not happen and consequently, no negative volume is produced during the solution. Using this method, there is no need to adapt the point to the point of the grid in the middle plane.



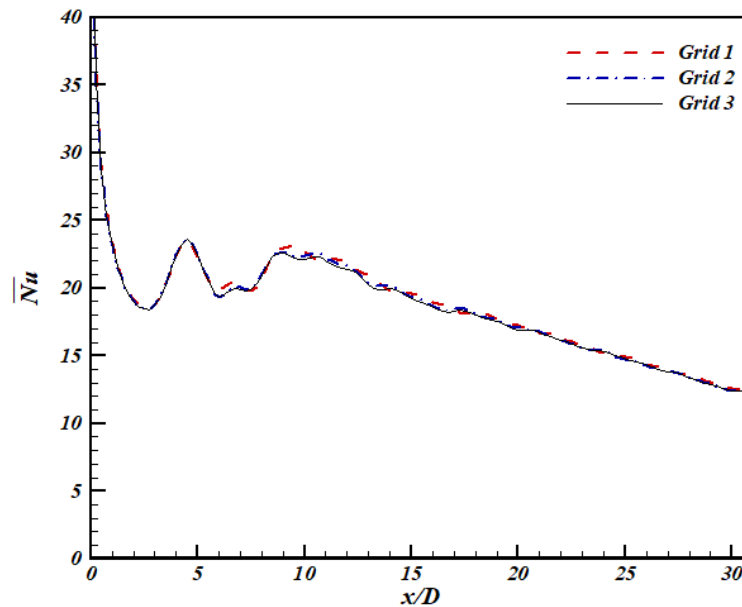


Fig. 4. Grid independence study for the stationary blade type +

### 3.2 Grid independence and results validation

The grid independence study was performed for three different grids with the number of structured elements 33820 (Grid 1), 49832 (Grid 2) and 59040 (Grid 3). The results were compared for the stationary blade type + at Reynolds number 100 and Prandtl number 1. The overall time averaged Nusselt number for these three grids was obtained 18.56, 18.68 and 18.73 respectively. Moreover, in Fig. 4, the wall time averaged Nusselt number along the channel was compared for the three above-mentioned grids. According to Fig. 4, it is observed that the results obtained from Grid 2 and Grid 3 are closed. Therefore, Grid 2 with the number of 49832 elements consisting of 9032 elements in the oscillating region and 40800 elements in the stationary region was chosen as the computational grid.

The present results for fourth different cases of fluid flow and heat transfer characteristics were compared with those presented in the literature. In the first validation case, the flow around a stationary heated circular cylinder at  $Re = 100$  and  $Pr = 0.7$  was studied. The values of Nusselt number  $Nu$ , Strouhal number  $St$ , drag coefficient  $C_d$  and lift coefficient  $C_l$  were compared with experimental [26, 27] and numerical [28, 29] results also with correlation obtained experimentally [30, 31] as reported in Table 1. In the second validation test case, the fluid flow characteristics around a rotating circular cylinder at  $Re = 100$  and different non-dimensional rotational velocity  $\alpha (= r\omega / U_\infty)$  were compared with the results presented in [32, 33] as shown in table 2. In the third validation test case, the verification was performed for flow around a circular cylinder confined in a channel at  $Re = 100$  and  $Pr = 1$  and the values of the local time averaged Nusselt number were compared with the values of the Nusselt number provided by Beskok et al. [19]. This validation and verification can be found in [21]. On the other hand, in order to validate the accuracy prediction of thermal behavior of the channel flow in the presence of an oscillating circular cylinder, the comparison was done with the numerical results presented by Beskok et al. [14] and Celik et al. [29]. In the present validation, the boundary conditions, flow conditions and geometric dimensions were completely matched to the simulated samples in [19] and [34]. Table 3 presents the comparison of the overall time averaged Nusselt number for different excitation frequencies  $F = f_e / f_0$  (where  $f_e$  and  $f_0$  are cylinder excitation and natural vortex shedding frequency, respectively) with a constant  $\theta = \pi / 4$  at  $Re = 100$  and  $Pr = 5.0$ . Comparison of present results with those in the related literature in fourth cases declares that the results are reliable and have acceptable levels of accuracy.

Table 1. Comparison of present results with those in the related literature

Source	Nu	St	$C_d$	$C_l$
Present study	5.16	0.167	1.38	$\pm 0.341$
Norberg [26]	-	0.168	-	$\pm 0.18$ to $\pm 0.54$
Tritton [27]	-	-	1.25	-
Mahir and Altaç [28]	$5.179 \pm 0.003$	0.172	$1.368 \pm 0.029$	$\pm 0.343$
kumar and Jayavel [29]	5.187	0.164	1.337	-
Knudsen and Katz [30]	5.19	-	-	-
Churchill and Bernstein [31]	5.16	-	-	-

Table 2. Comparison of present results with those in the related literature








Source	$\alpha = 0$		$\alpha = 1$		$\alpha = 2$	
	$C_l$	$C_d$	$C_l$	$C_d$	$C_l$	$C_d$
Present study	0	1.355	-2.523	1.135	-5.535	0.493
Stajkovic et al. [32, 33]	0	1.36	-2.46	1.1	-5.47	0.47



**Table 3.** Comparison of present results with those in the related literature

Source	Nu		
	F = 0.5	F = 0.75	F = 1
Present study	26.57	28.84	27.58
Beskok et al. [19]	28.83	31.58	29.60
Celik et al. [34]	-	24.43	-

**Table 4.** Description of studied cases

Case no.	Situation	Shape of the blade
1	Stationary blade (SB1)	
	Oscillating blade (OB1), $\theta = \pi/6, \pi/4$ , rpm = 300, 600	
2	Stationary blade (SB2)	
	Oscillating blade (OB2), $\theta = \pi/6, \pi/4$ , rpm = 300, 600	
3	Stationary blade (SB3)	
	Oscillating blade (OB3), $\theta = \pi/6, \pi/4$ , rpm = 300, 600	
4	Stationary blade (SB4)	
	Oscillating blade (OB4), $\theta = \pi/6, \pi/4$ , rpm = 300, 600	
5	Stationary blade (SB5)	
	Oscillating blade (OB5), $\theta = \pi/6, \pi/4$ , rpm = 300, 600	
6	Stationary blade (SB7)	
	Oscillating blade (OB7), $\theta = \pi/6, \pi/4$ , rpm = 300, 600	
7	Stationary blade (SB7)	
	Oscillating blade (OB7), $\theta = \pi/6, \pi/4$ , rpm = 300, 600	

<sup>1</sup>Data is from [21]

## 4. Results and Discussion

### 4.1 Description of cases

As previously mentioned, to investigate the heat transfer enhancement, 35 states were studied numerically including cases 1 to 7, which compared with straight channel under the same boundary conditions (see Table 4). In order to investigate the effect of generated vortices due to the presence of blades on the wall thermal boundary layer and as a result of the heat transfer, the local time averaged Nusselt number is studied.

In Fig. 5, the local time averaged Nusselt number over  $0 \leq t \leq \tau/2$  for both upper and lower surfaces of the channel and the local time averaged Nusselt number over  $0 \leq t \leq \tau$  are presented for OB2 with rpm = 600. As it can be seen, the Nusselt number oscillates at both upper and lower surfaces. These Nusselt number variations are related to the effects of vortices that are generated in the direction of the flow behind the oscillating blades. When the vortex flow approaches the upper wall, the thickness of the thermal boundary layer decreases and the Nusselt number increases. At this time, the thickness of the thermal boundary layer on the lower wall increases, and as a result, the Nusselt number decreases. This process is frequently repeated. In other words, the instantaneous Nusselt number profile for the upper and lower walls has a phase lag. The oscillations amplitude of the Nusselt number along the flow decreases, since the size of the vortex is diminished due to the dissipation. The first increase in the Nusselt number is related to the location of the blades and does not correlate with the vortices separated from the body. At the blades location, the cross-sectional area of the flow decreases and the fluid velocity increases, which results in reducing the thickness of the boundary layer and increasing the Nusselt number. This increase is also visible in all subsequent figures.

### 4.2 Results of case 2

Figure 6 (a) to (c) indicates the distribution of vorticity  $\zeta$  and non-dimensional temperature  $T^*$  respectively for the straight channel and channel with SB2 and OB2. As it can be seen in Fig. 6 the thermal boundary layer starts to grow along the flow through the channel. According to Fig. 6 (b) for stationary blades, both blades are perpendicular to the fluid flow path, which minimizes the cross-sectional area of the flow and increases the flow velocity. In this figure, the flow separation and vortex shedding (with the positive and negative rotations) are visible. Vortices move toward the wall that results in reducing the thickness of the thermal boundary layer. Moreover, the movement of the vortex toward the wall results in moving cool fluid from the channel center to the wall and mixing of cold and hot flows, which can have a positive effect on the increase of heat transfer. Figure 6 (c) shows the flow on the oscillating blades with  $\theta = \pi/4$  and rpm = 600, respectively. As it can be observed, in this case there is a vortex flow as well, but the difference is that the vortices have been stretched more than the stationary blades, its separation time has increased and the pattern of shedding has changed. Because of the blades oscillation, the rate of blockage and the angle of separation of the flow have been changed, and the effect of the blades on generation of vortex flow decreases. In comparison with the stationary state, due to the weakening of the vortices, the thermal boundary layer is less affected from the vortices. These differences are recognizable from the comparison of Fig. 6 (b) and (c). So, it seems that the stationary blades have a greater influence on the increase in heat transfer.



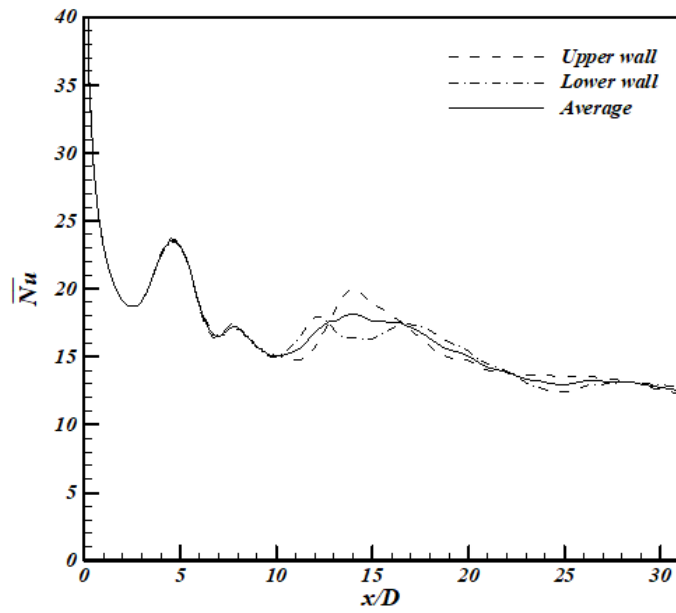


Fig. 5. Local time averaged Nusselt number for upper and lower walls and local time averaged Nusselt number of the channel with OB2.

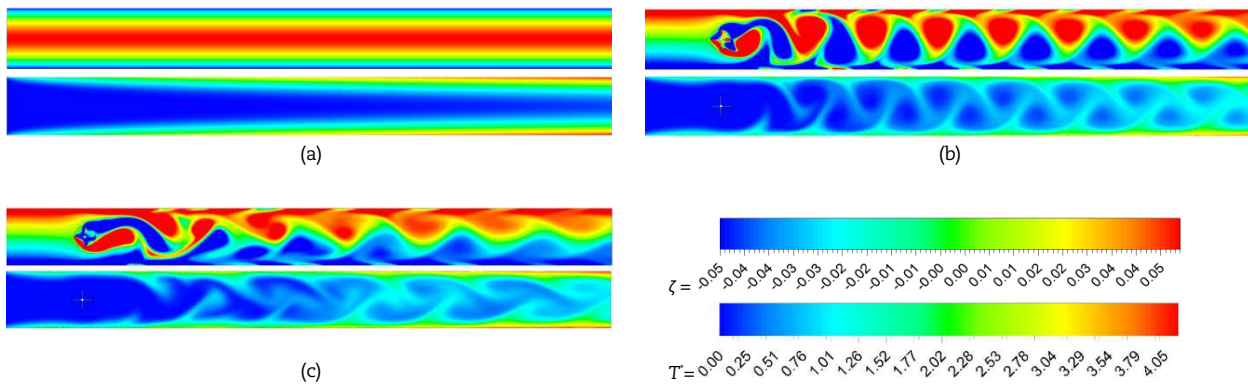


Fig. 6. Vorticity and temperature contours (a) straight channel and channel with (b) SB2 and (c) OB2 at  $rpm = 600$  and  $\theta = \pi / 4$  ( $T^* = (T - T_{in}) / (T_b - T_{in})$ ).

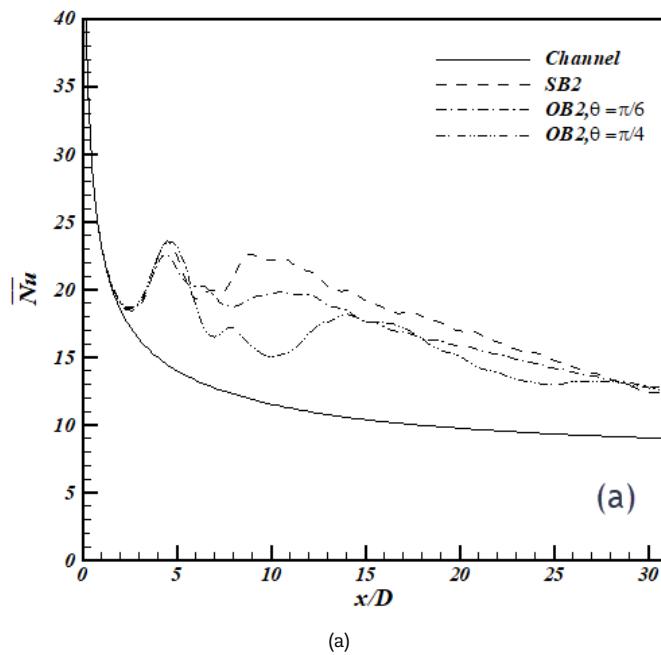


Fig. 7. Variations of the time averaged Nusselt number of the channel with SB2 and OB2 at  $rpm =$  (a) 600 and (b) 300.



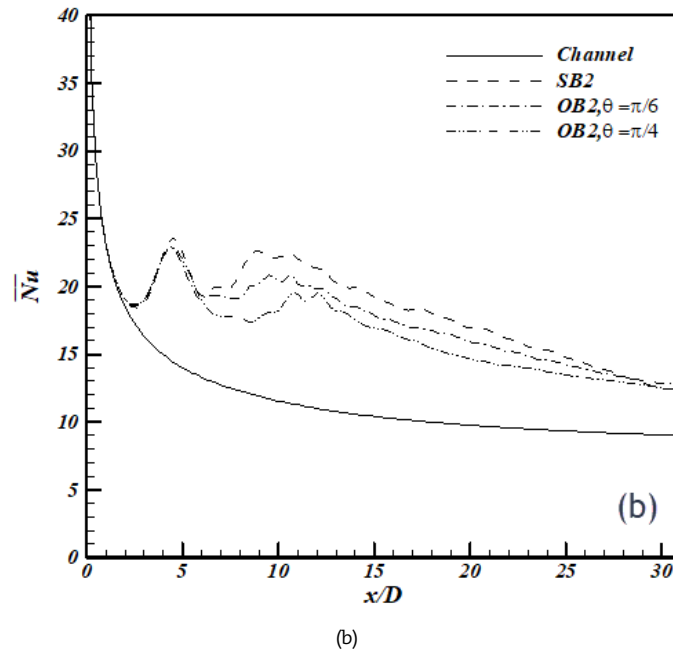


Fig. 7. Continued.

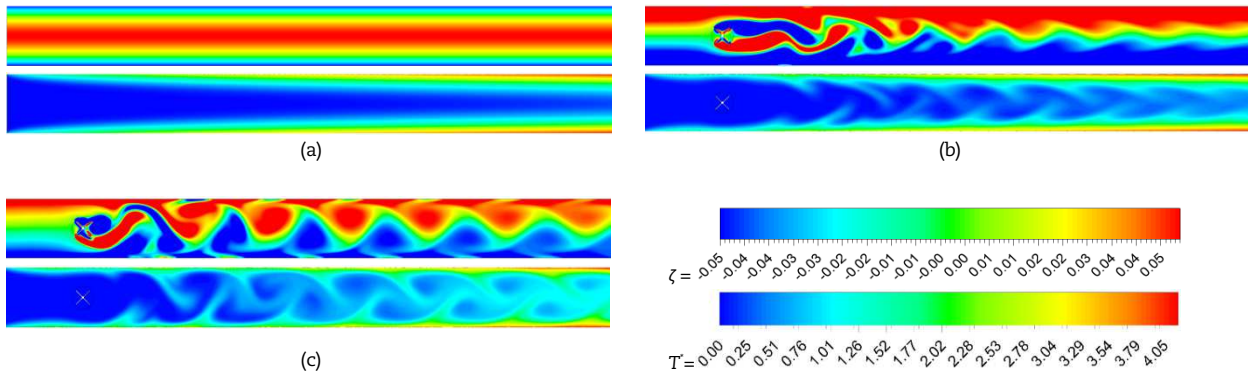


Fig. 8. Vorticity and temperature contours (a) straight channel and channel with (b) SB3 and (c) OB3 at  $rpm = 600$  and  $\theta = \pi / 4$ .

Figure 7 (a) and (b) indicate variations of the time averaged Nusselt number over the straight channel and channel with SB2 and OB2 with  $\theta = \pi / 4$  and  $\pi / 6$ , also  $rpm = 600$  and  $300$ . In the straight channel, while boundary layer growing along the channel, the local Nusselt number decreases uniformly. According to this figure, there are several increments in the Nusselt number curve. The first increase is the same for almost all states and is related to the location of the blades. Further increases are due to the effect of vortices on the surface and the separation of the boundary layer from the channel wall. In all cases, the use of the blades enhances the heat transfer with respect to the straight channel. The maximum heat transfer rate is related to the stationary blades, since according to Fig. 6 the blades oscillation makes the vortices weaker and its effect on the boundary layer becomes lower, and consequently the heat transfer rate is less enhanced. Also, from the comparison of Fig. 7 (a) and (b), it can be said that by increasing oscillating speed, the difference between the Nusselt number curves is increased in different cases. For  $\theta = \pi / 4$  and  $rpm = 600$ , due to stretching the vortex, its effect on the wall and the separation of the wall boundary layer, and finally increasing the local Nusselt number occurs far away, that as oscillation speed decreases the stretching the vortices decreases and the position of local increase becomes closer to the blades.

4.3 Results of case 3

Figure 8 (a) to (c) shows the vorticity and temperature contours for the straight channel and the channel with equipped with SB3 and OB3. As it can be seen, the shape and pattern of vortex shedding for SB2 (Fig. 6 (b)) and SB3 (Fig. 8 (b)) are completely different. For the stationary blades, according to their position in the flow, the flow separation occurs from the front and behind the blades. The vortices formed behind the blades are stretched and quickly disappeared in the flow and has no significant effect on the boundary layer. This indicate the importance of the blades position in the flow. In the oscillatory state, the vortex stretching decreases, and it takes more distance to destroy. These vortices also move toward the wall and have a greater impact on the boundary layer. Blades oscillation increase the flow obstruction and vortex shedding becomes faster. Figure 9 (a) and (b) compare variation of the time-averaged Nusselt number over the straight channel and channel with SB3 and OB3 for  $\theta = \pi / 4$  and  $\pi / 6$  and  $rpm = 600$  and  $300$ . As can be seen, the maximum Nusselt number is related to the oscillating blades with  $\theta = \pi / 4$  and  $rpm = 600$ . Of course, according to Fig. 8, this was predictable. Unlike OB2 in OB3, oscillation helps





enhancing heat transfer with respect to the stationary case. Therefore, the blades position in the channel can have a significant effect on the heat transfer. The blades oscillation with  $\theta = \pi / 4$  and  $rpm = 600$ , in addition to the overall effect, have significant local effects on the Nusselt number and the enhancement in heat transfer. But in SB3 case, the results related to the part of the end of the channel are closer to the results of the straight channel, which indicates the thermal boundary layer growth.

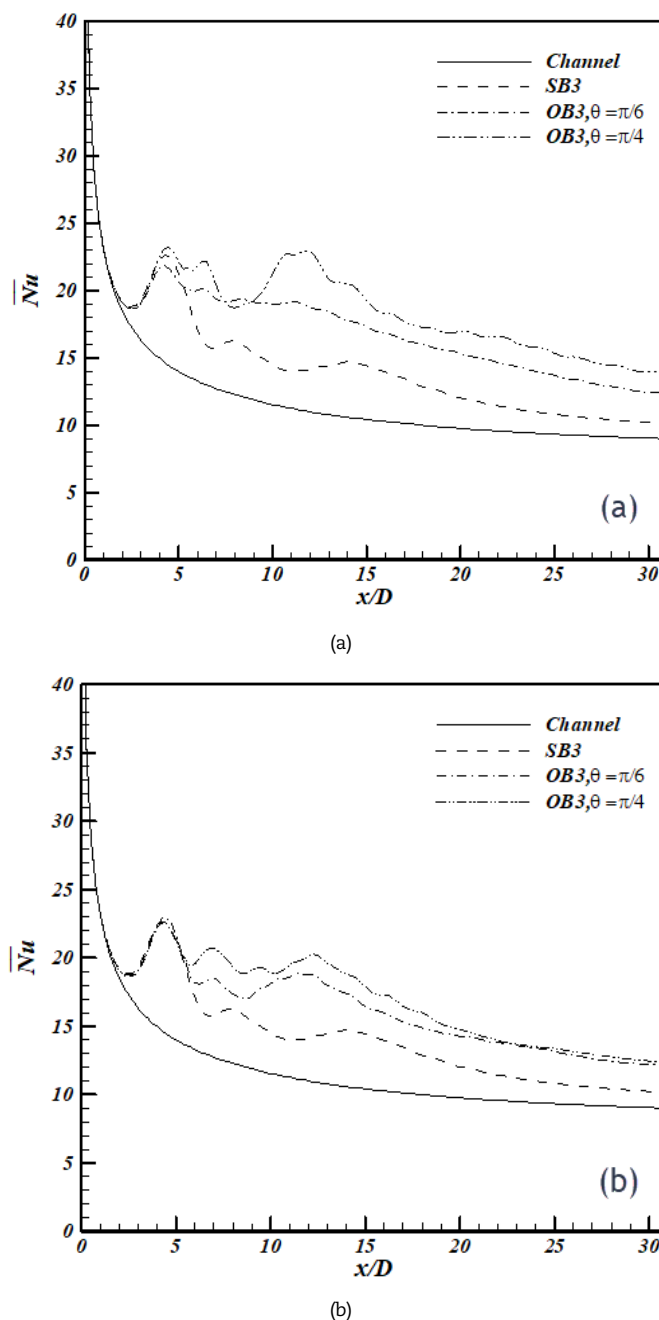


Fig. 9. Variations of the time-averaged Nusslet number of the channel with SB3 and OB3 at  $rpm =$  (a) 600 and (b) 300

#### 4.4 Results of case 4

Figure 10 (a) to (c) indicates the vorticity and temperature contours for the straight channel and the channel in the presence of SB4 and OB4. In this case, the number of blades is 6. Flow separation (from the first and the last blades) and vortex shedding have occurred for the stationary blades, but in comparison with the oscillating state, vortices are weaker and less effective on the boundary layer. Comparing Figs 6, 8, and 10 exhibits that changing the blades geometry affects the vortex shedding pattern. In Fig. 10, it is seen that after the blades, the vortices are separated from the surface. In addition, the vortices generated by the blades hit the surface which complicates the flow behavior analysis. Therefore, at first behind the blades, two vortices with the same direction and one vortex in opposite direction are visible. In the flow path, the two vortices with the same direction are merged, and eventually they disappear through the flow due to dissipation. Figure 11 compares variations of the time-averaged Nusslet number over the straight channel and channel with SB4 and OB4 for  $\theta = \pi / 4$  and  $\pi/6$ , and  $rpm = 600$  and 300. As it can be seen and predicted from the contours, the maximum Nusselt number is related to the channel equipped with the oscillating blades with  $\theta = \pi / 4$  and  $rpm = 600$ . In this case, increasing the oscillating speed, increases the results differences.



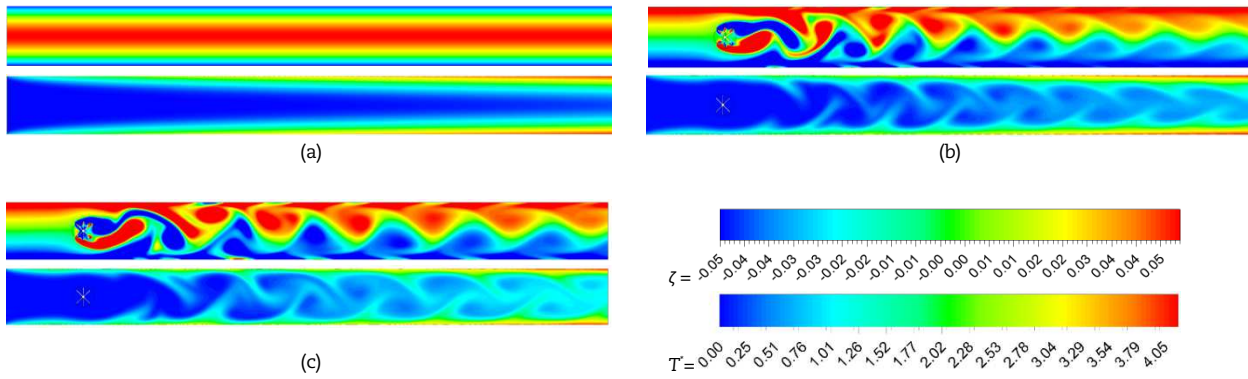
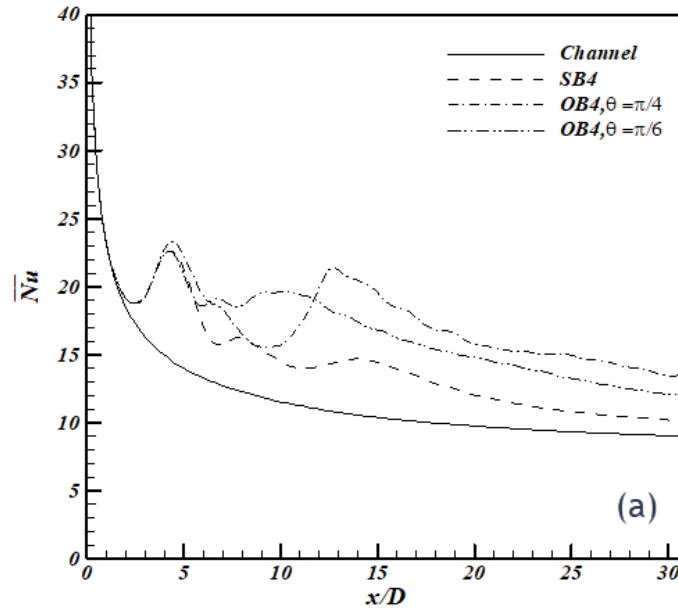
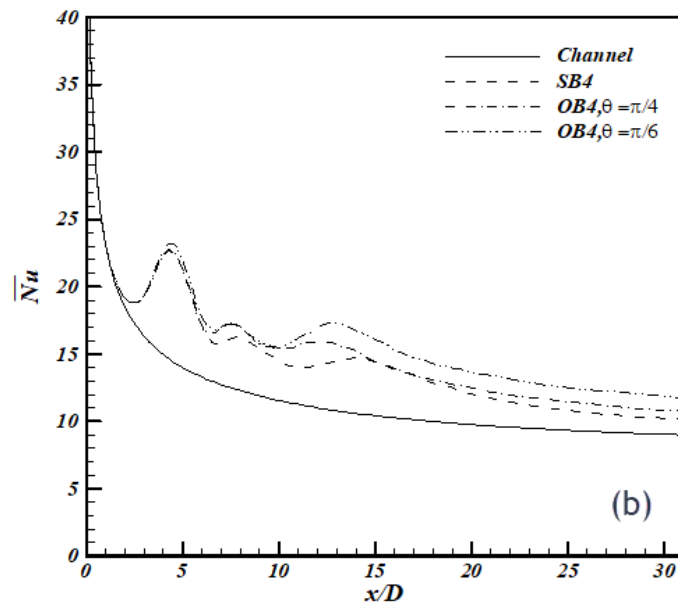


Fig. 10. Vorticity and temperature contours (a) straight channel and channel with (b) SB4 and (c) OB4 at  $rpm = 600$  and  $\theta = \pi / 4$ .



(a)



(b)

Fig. 11. Variations of the time averaged Nusslet number of the channel with SB4 and OB4 at  $rpm =$  (a) 600 and (b) 300

4.5 Results of case 5

Figure 12 shows the vorticity and temperature contours for the straight channel and the channel equipped with SB4 and OB4. In this case, the number of blades is 6 as well, but its layout has been changed compared to the previous one.



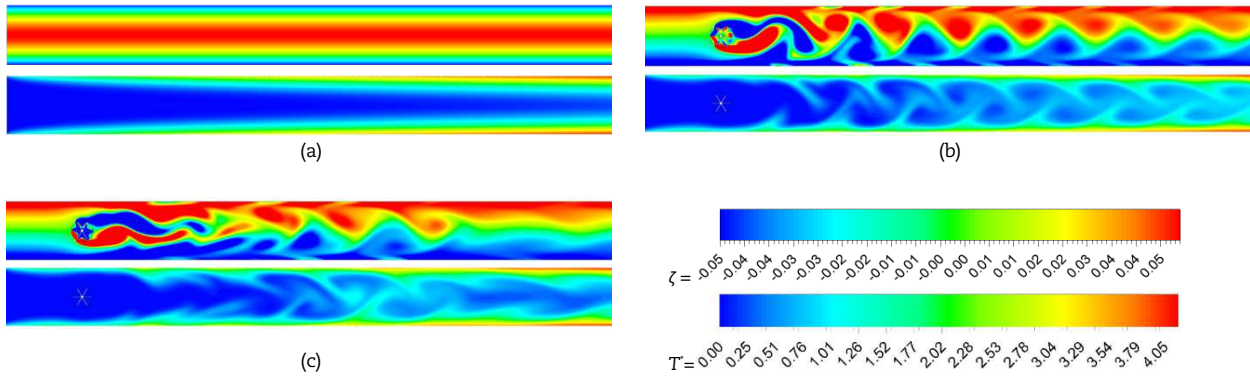


Fig. 12. Vorticity and temperature contours (a) straight channel and channel with (b) SB5 and (c) OB5 at  $rpm = 600$  and  $\theta = \pi / 4$

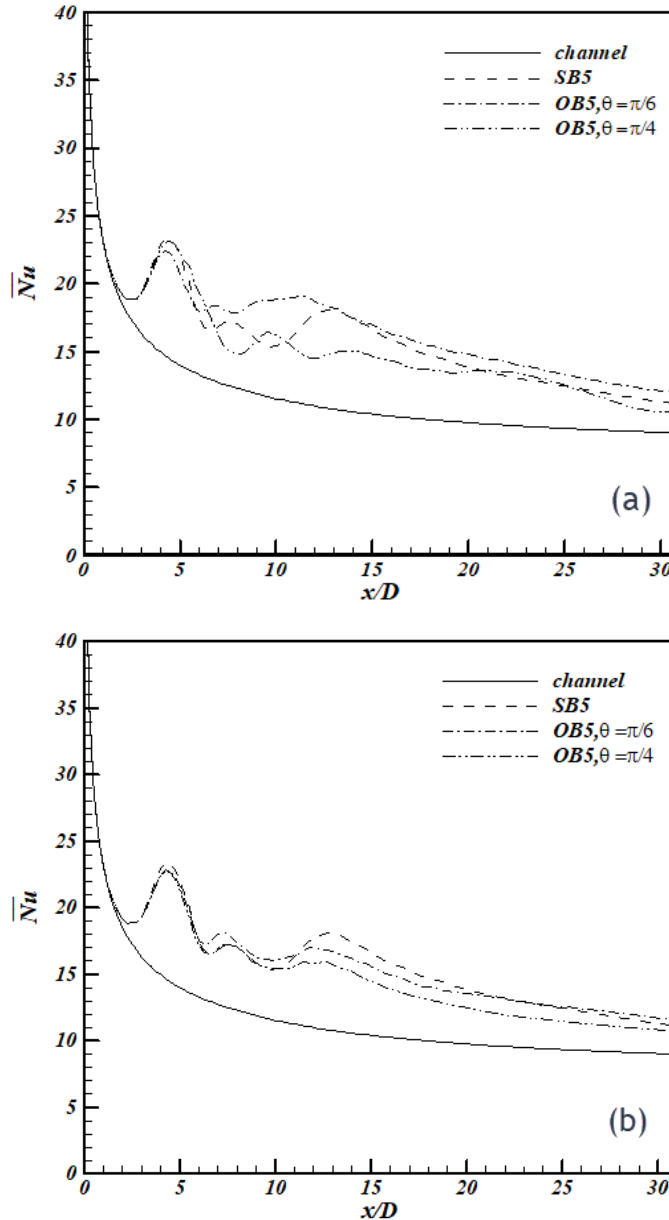


Fig. 13. Variations of the time averaged Nusslet number of the channel with SB5 and OB5 at  $rpm =$  (a) 600 and (b) 300

It can be seen that vortex shedding occurs in the stationary blades, but this phenomenon becomes weaker due to the blades oscillation. In addition, the blades oscillation causes irregularity in the separation pattern and flow on the wall. Figure 13 compares variations of the time averaged Nusselt number over the straight channel and channel with SB5 and OB5 for  $\theta = \pi / 4$  and  $\pi / 6$ , and  $rpm = 600$  and 300. As it can be seen, the maximum Nusselt number is related to the oscillating blades with  $\theta = \pi / 6$  and  $rpm = 600$ . It can be observed that changing the blades layout from SB4 to SB5 could help heat transfer enhancement. Of course, the Nusselt number in the OB4 case is more than OB5, which is due to more flow obstruction in OB4 at both oscillation angles with respect to OB5.



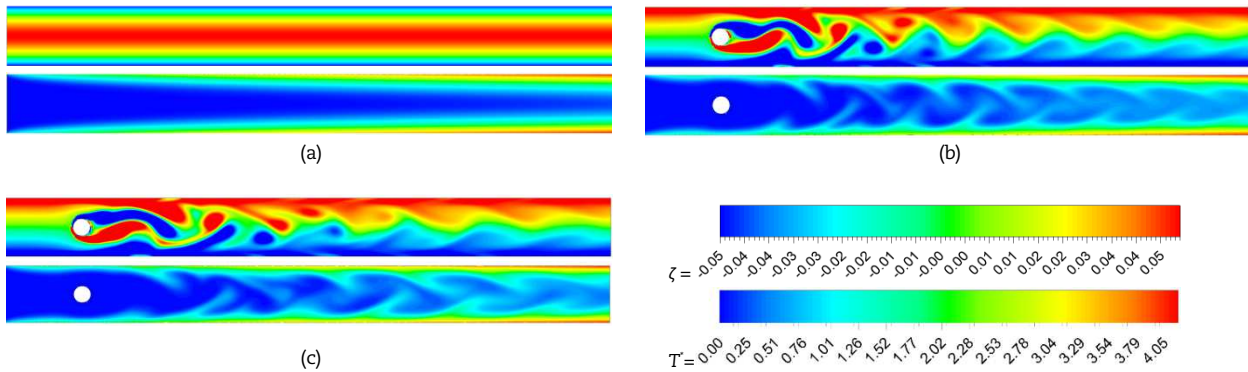


Fig. 14. Vorticity and temperature contours (a) straight channel and channel with (b) SB7 and (c) OB7 at  $rpm = 600$  and the  $\theta = \pi / 4$

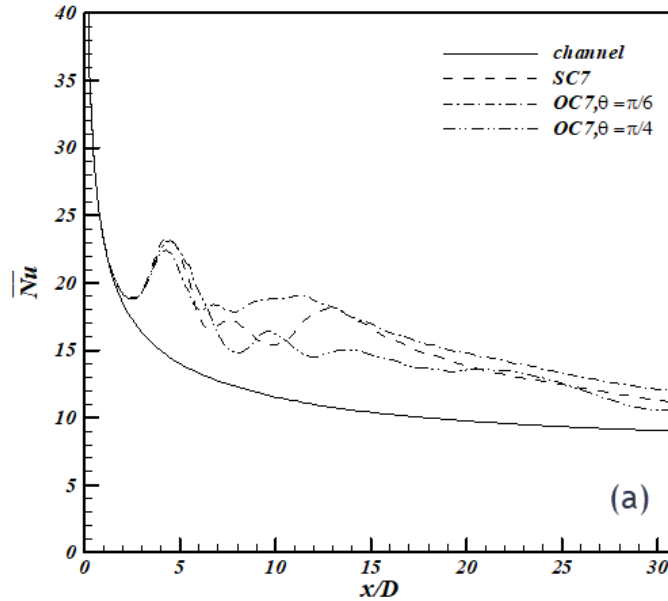


Fig. 15. Variations of the time averaged Nusslet number of the channel with SB7 and OB7 at  $rpm =$  (a) 600 and (b) 300

4.6 Results of case 7

Figure 14 indicates the vorticity and temperature contours for the straight channel and the channel in the presence of SB7 and OB7. In this case, the blades with height of  $1/8D$  are located on a circular cylinder with a diameter of  $7/8D$ . In both stationary and oscillating cases, the vortex shedding is weakened and does not have any significant influence on the thermal boundary layer. Moreover, the vortex shedding pattern is similar to each other. Therefore, the blades height can affect the heat transfer enhancement. In Fig. 15, variations of the time averaged Nusslet number over the straight channel and channel equipped with SB5 and OB5 for  $\theta = \pi / 4$  and  $\pi/6$ , also  $rpm = 600$  and  $300$  are presented. Due to the similarity of the vortex shedding pattern, the variation of the Nusselt number is similar at  $rpm = 300$ , but with increasing oscillating speed, this pattern changes slightly, which results in some differences between the results.

4.7 Comparison of cases

Inserting actuators or blades are specifically effective for heat transfer enhancement in meso-scale channels such as micro-heat exchangers. However, it is evident that inserting a blade results in a pressure drop penalty, but, in such cases, the main purpose is to enhance the heat transfer. In this section, the main objective is to show that the thermal and hydraulic performances of the blades are directly dependent on the state and shape of the blade. It is shown that the shape and state of blades can influence the pressure drop remarkably and restricts their applications for the thermal systems working under limited pumping power conditions, such as the case for electronic cooling. Therefore, the designer can select the blade shape and state based on these results.

First, to investigate more precisely the effect of blades number and angular velocity of the oscillation on the heat transfer enhancement, in Fig. 16, the total time-averaged Nusselt number ( $\overline{Nu}$ ) with respect to the averaged Nusselt number of the straight channel ( $Nu_c$ ) is plotted for different oscillating speeds and oscillation angles, in which  $Nu_r = \overline{Nu} / Nu_c$ . In this figure, the results of the channel equipped with stationary blade type  $\blacksquare$  (SB1), oscillating blade type  $\blacksquare$  (OB1), stationary cylinder SC6), and oscillating cylinder (OC6) [21] are presented as well. As shown in Fig. 16, the maximum increase in Nusselt number with respect to the straight channel is 63.8% and is related to the channel with SB1. The minimum heat transfer enhancement is related to the channel with SB7 and OC6 and is about 19%. The maximum effect of the oscillation angle on the increase of Nusselt number with respect to the stationary state is observed for case OB3 with  $\theta = \pi / 4$  which is about 42%.



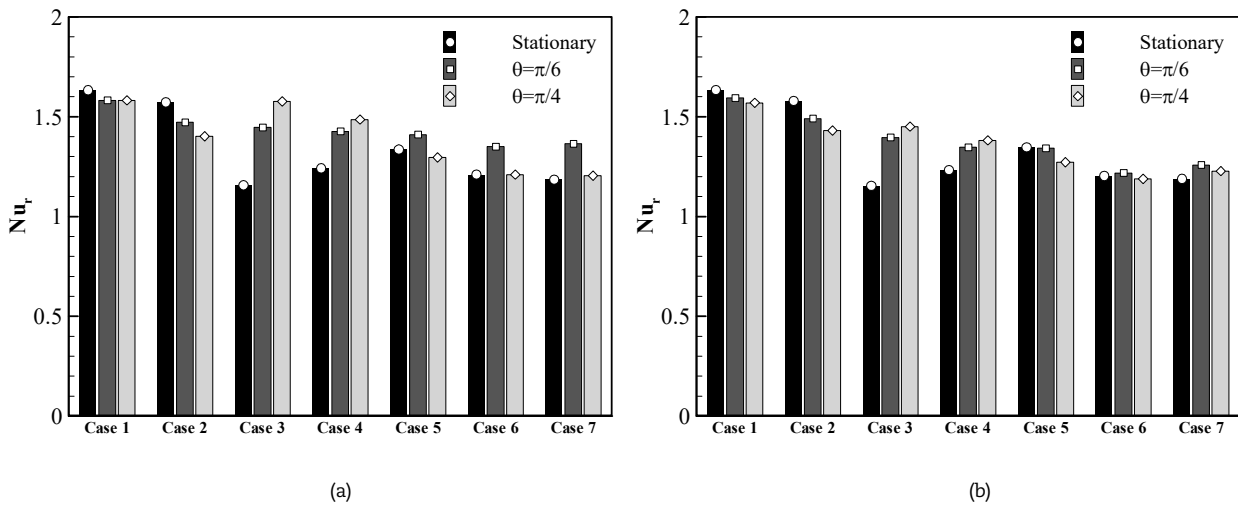


Fig. 16. Comparing the total time-averaged Nusselt number ( $\overline{Nu}$ ) of the channel in the presence of various blades layouts with respect to the averaged Nusslet number of the straight channel ( $Nu_c$ ) at  $rpm =$  (a) 600 and (b) 300

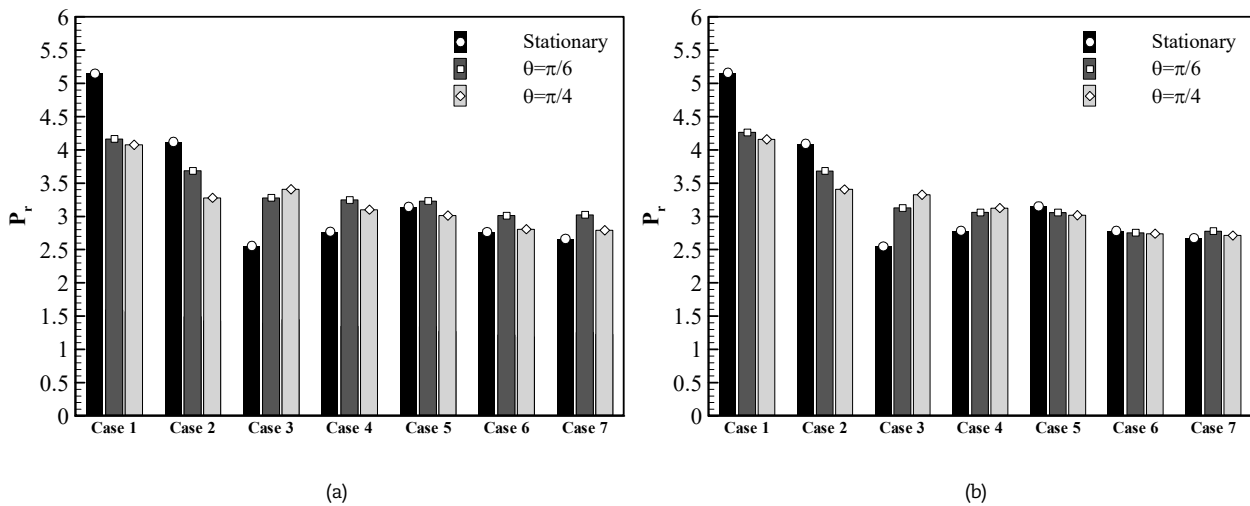


Fig. 17. Channel pressure drop with different blades layouts with respect to the straight channel at  $rpm =$  (a) 600 and (b) 300

The effect of the oscillating speed is significant for OC6 and OB7 cases with  $\theta = \pi / 4$ . Adding the blades to the cylinder and their transformation into SB7/OB7 case did not have much effect on the heat transfer enhancement with respect to the SC6/OC6. Comparing the results of blades with different layouts, it can be concluded that the number of blades has a great influence on the heat transfer.

Putting the blades in the channel, in addition to the heat transfer enhancement, will increase the pressure drop. The channel pressure drop with different blades with respect to the straight channel is shown in Fig. 17. In this figure, the results for SB1, OB1, SC6 and OC6 [21] are also presented. According to the figure, it can be seen that the maximum pressure drop is related to the channel with SB1 and the minimum pressure drop is related to the channel with SB3. According to Fig. 17, the variation of the oscillation angle of the OB1 at  $rpm = 600$  has the maximum (about 110%) and of the OB6 at  $rpm = 300$ , the minimum (about 3%) effect in reducing the pressure drop. It was also observed that adding short blades to the cylinder (SB7/OB7) does not affect the blockage of flow and vortex shedding pattern with respect to the SC6/OC6, and so the pressure drop of these cases is close to each other.

### 5. Conclusion

In this paper, the heat transfer enhancement in the presence of blades with different geometries and oscillating conditions for a Reynolds number of 100 was numerically investigated. In order to investigate the rate of the heat transfer enhancement, variation of time-averaged Nusslet number for an oscillating case with  $\theta = \pi / 6$  and  $\pi / 4$  and  $rpm = 300$  and 600 was investigated. The sliding mesh method was utilized to simulate the oscillating blades. The results indicated that :

- ❖ The heat transfer from the channel with the blade type + in the stationary state was more than the blade type ✕. The oscillation of blades ✕ increased the heat transfer relative to the stationary state while this trend was opposite for the blade +.
- ❖ For the blade type ✱, the oscillation enhanced the heat transfer relative to the stationary state. This process was the opposite in most cases of the blade type ✱.
- ❖ The results showed that adding the blades to the cylinder does not have much influence on the heat transfer enhancement with respect to the cylinder.



- ❖ The maximum heat transfer and pressure drop among the different geometries of the blades were related to type **I** in the stationary state. The minimum heat transfer enhancement and pressure drop were related to the type **X** in the stationary state.
- ❖ In most cases, the effect of the oscillation angle is greater than the oscillating speed on heat transfer enhancement.
- ❖ Increasing the number of blades did not necessarily help to enhance the heat transfer, but it could affect the decrease in pressure drop.
- ❖ The blades configuration in flow had a great influence in the vortex shedding pattern, vortex strength, heat transfer rate, and pressure drop.
- ❖ The presence of the blades and their oscillation, in addition to the overall effect on the heat transfer enhancement, had effects on the local heat transfer enhancement.
- ❖ The best thermo-hydraulic performance was related to OB3 for  $\theta = \pi / 4$  and  $rpm = 600$ .

### Author Contributions

E. Izadpanah and M.H. Hekmat planned the computational framework and analysed the data. M. Yazdanian and Y. Amini performed the numerical calculations. E. Izadpanah and M. Yazdanian wrote the manuscript with input from all authors. All authors discussed the results, reviewed and approved the final version of the manuscript.

### Acknowledgments

Not applicable.

### Conflict of Interest

The authors declared no potential conflicts of interest with respect to the research, authorship and publication of this article.

### Funding

The authors received no financial support for the research, authorship and publication of this article.

### Data Availability Statements

The datasets generated and/or analyzed during the current study are available from the corresponding author on reasonable request.

### Nomenclature

$D$	Blockage length of blade [ m ]	$Re$	Reynolds number
$k$	Thermal conductivity [ W / m .K ]	$St$	Strouhal number
$Nu$	Nusselt number	$t$	Time [ s ]
$Nu_c$	Nusselt number of the straight channel	$T$	Temperature [ K ]
$Nu_r$	Normalized Nusselt number = $\overline{Nu} / Nu_c$	$T_b$	Bulk temperature [ K ]
$\overline{Nu}$	Time averaged Nusselt number	$T_w$	Wall temperature [ K ]
$\overline{Nu}$	Total time averaged Nusselt number	$\zeta$	Vorticity [ 1 / s ]
$p$	Pressure [ Pa ]	$\theta$	The maximum oscillation angle [ rad ]
$P_r$	Normalized pressure drop ( = $\Delta p / \Delta p_c$ )	$\mu$	Dynamic viscosity [ N.s / m <sup>2</sup> ]
$Pr$	Prandtl number	$\rho$	Density [ kg / m <sup>3</sup> ]
$q''$	Heat flux ( W / m <sup>2</sup> )		



### References

- [1] Ali M.M., Alim M.A., Ahmed S.S., Oriented magnetic field effect on mixed convective flow of nanofluid in a grooved channel with internal rotating cylindrical heat source, *International Journal of Mechanical Sciences*, 151, 2019, 385-409.
- [2] Yang Y., Li H., Yao M., Gao W., Zhang Y., Zhang L., Investigation on the effects of narrowed channel cross-sections on the heat transfer performance of a wavy-channeled PCHE, *International Journal of Heat and Mass Transfer*, 135, 2019, 33-43.
- [3] Gustafsson A., Analysis of Vortex-Induced Vibrations of Risers, Master's thesis, Department of Applied Mechanics, Chalmers University of Technology, Gothenburg, Sweden, 2012.
- [4] Munish G., Kasana S.K., Vasudevan R., Heat transfer augmentation in a plate-fin heat exchanger using rectangular winglet, *Journal of Heat Transfer—Asian Research*, 39(8), 2010, 590 – 610.
- [5] Pauley W.R., Eaton J.K., The effect of embedded longitudinal vortex array on turbulent boundary layer heat transfer, *Journal of Heat Transfer*, 116, 1994, 871-885.
- [6] Amini Y., Akhavan S., Izadpanah E., A numerical investigation on the heat transfer characteristics of nanofluid flow in a three-dimensional microchannel with harmonic rotating vortex generators, *Journal of Thermal Analysis and Calorimetry*, 139, 2020, 755-764.
- [7] Mohammadshahi S., Nili-Ahmadabadi M., Samsam-Khayani H., Salimpour M.R., Numerical study of a vortex-induced vibration technique for passive heat transfer enhancement in internal turbulent flow, *European Journal of Mechanics / B Fluids*, 72, 2018, 103-113.
- [8] Hekmat M.H., Ziarati K.K., Effects of nanoparticles volume fraction and magnetic field gradient on the mixed convection of a ferrofluid in the annulus between vertical concentric cylinders, *Applied Thermal Engineering*, 152, 2019, 844-857.



- [9] Hekmat M. H., Rabiee M. B., Ziarati K. K., Numerical investigation of the mixed convection of a magnetic nanofluid in an annulus between two vertical concentric cylinders under the influence of a non-uniform external magnetic field, *Journal of Thermal Analysis and Calorimetry*, 138, 2019, 1745-1759.
- [10] Liang G., Mudawar I., Review of single-phase and two-phase nanofluid heat transfer in macro-channels and micro-channels, *International Journal of Heat and Mass Transfer*, 136, 2019, 324-354.
- [11] Izadpanah E., Amini Y., Ashouri A., A comprehensive investigation of vortex induced vibration effects on the heat transfer from a circular cylinder, *International Journal of Thermal Sciences*, 125, 2018, 405-418.
- [12] Izadpanah E., Ashouri A., Liravi M., Amini Y., Effect of vortex-induced vibration of finned cylinders on heat transfer enhancement, *Physics of Fluids*, 31, 2019, 073604.
- [13] Amini Y., Akhavan S., Izadpanah E., Vortex-induced vibration of a cylinder in pulsating nanofluid flow, *Journal of Thermal Analysis and Calorimetry*, 140, 2020, 2143-2158.
- [14] Khan M.I., Billah M.M., Rahman M.M., Hasan M.N., Mixed convection heat transfer simulation in a rectangular channel with a variable speed rotational cylinder, *AIP Conference Proceedings*, 1919(1), 2017, 020048.
- [15] Esmaeilzadeh E., Alamgholilou A., Mirzaie H., Ashna M., Heat transfer enhancement in the presence of an electric field at low and intermediate Reynolds numbers, *Asian Journal of Scientific Research*, 1(6), 2008, 562-578.
- [16] Eid E.I., Gomaa M.E., Influence of vibration in enhancement of heat transfer rates from thin planar fins, *Heat and Mass Transfer*, 45, 2009, 713-726.
- [17] Raguraman C.M., Ragupathy A., Ramkumar R., Sivakumar L., An effect of blade geometry on heat transfer performance in stirred vessel-coal water slurry system using coal gasification, *International Journal of Engineering Science and Technology*, 2, 2010, 587-594.
- [18] Page L.G., Bello-Ochende T., Meyer J.P., Maximum heat transfer density rate enhancement from cylinders rotating in natural convection, *International Communications in Heat and Mass Transfer*, 38, 2011, 1354-1359.
- [19] Beskok A., Raisee M., Celik B., Yagiz B., Cheraghi M., Heat transfer enhancement in a straight channel via a rotationally oscillating adiabatic cylinder, *International Journal of Thermal Sciences*, 58, 2012, 61-69.
- [20] Léal L., Miscevic M., Lavieille P., Amokrane M., Pigache F., Topin F., Nogarède B., Tadriss L., An overview of heat transfer enhancement methods and new perspectives: Focus on active methods using electroactive materials, *International Journal of Heat and Mass Transfer*, 61, 2013, 505-524.
- [21] Pourgholam M., Izadpanah E., Motamedi R., Habibi S.E., Convective heat transfer enhancement in a parallel plate channel by means of rotating or oscillating blade in the angular direction, *Applied Thermal Engineering*, 78, 2015, 248-257.
- [22] Yeom T., Simon T.W., North M., Cui T., High-frequency translational agitation with micro pin-fin surfaces for enhancing heat transfer of forced convection, *International Journal of Heat and Mass Transfer*, 94, 2016, 354-365.
- [23] Izadpanah E., Babaie Rabiee M., Sadeghi H., Talebi S., Effect of rotating and oscillating blade on the heat transfer enhancement of non-Newtonian fluid flow in a channel, *Applied Thermal Engineering*, 113, 2017, 1277-1282.
- [24] Kankariya D., Briens C., Pjontek D., Tacchino S., Effects of liquid feed rate and impeller rotation speed on heat transfer in a mechanically fluidized reactor, *Particuology*, 39, 2018, 25-32.
- [25] ANSYS CFX-Solver Theory Guide, Release 14.0, ANSYS Inc, 2013.
- [26] Norberg C., Fluctuating lift on a circular cylinder: review and new measurements, *Journal of Fluids and Structures*, 17, 2003, 57-96.
- [27] Tritton D.J., Experiments on the flow past a circular cylinder at low Reynolds numbers, *Journal of Fluid Mechanics*, 6, 1959, 547-567.
- [28] Mahir N., Altaç Z., Numerical investigation of convective heat transfer in unsteady flow past two cylinders in tandem arrangements, *International Journal of Heat and Fluid Flow*, 29(5), 2008, 1309-1318.
- [29] Kumar R.S., Jayavel S., Influence of flow shedding frequency on convection heat transfer from bank of circular tubes in heat exchangers under cross flow, *International Journal of Heat and Mass Transfer*, 105, 2017, 376-393.
- [30] Knudsen J.G., Katz D.L., *Fluid dynamics and heat transfer*, Chem. Eng. Ser. McGraw-Hill, New York, NY, 1958.
- [31] Churchill S.W., Bernstein M., A correlating equation for forced convection from gases and liquids to a circular cylinder in crossflow, *Journal of Heat Transfer*, 99, 1977, 300-306.
- [32] Stojković D., Breuer M., Durst F., Effect of high rotation rates on the laminar flow around a circular cylinder, *Physics of Fluids*, 14, 2002, 3160-3178.
- [33] Stojković D., Schön P., Breuer M., Durst F., On the new vortex shedding mode past a rotating circular cylinder, *Physics of Fluids*, 15, 2003, 1257-1260.
- [34] Celik B., Raisee M., Beskok A., Heat transfer enhancement in a slot channel via a transversely oscillating adiabatic circular cylinder, *International Journal of Heat and Mass Transfer*, 53, 2010, 626-634.

## ORCID iD

Ehsan Izadpanah  <https://orcid.org/0000-0003-2947-5766>  
 Milan Yazdaniyan  <https://orcid.org/0000-0003-1568-4794>  
 Mohamad Hamed Hekmat  <https://orcid.org/0000-0002-7059-6247>  
 Yasser Amini  <https://orcid.org/0000-0001-9006-9711>



© 2020 by the authors. Licensee SCU, Ahvaz, Iran. This article is an open access article distributed under the terms and conditions of the Creative Commons Attribution-NonCommercial 4.0 International (CC BY-NC 4.0 license) (<http://creativecommons.org/licenses/by-nc/4.0/>).

**How to cite this article:** Izadpanah E., Yazdaniyan M., Hekmat M.H., Amini Y. Thermal Performance of Oscillating Blade with Various Geometries in a Straight Channel, *J. Appl. Comput. Mech.*, 8(1), 2022, 114-128.  
<https://doi.org/10.22055/JACM.2020.31803.1919>

**Publisher's Note** Shahid Chamran University of Ahvaz remains neutral with regard to jurisdictional claims in published maps and institutional affiliations.

